

## LETTERS

### Diffusion-Driven Front Instability in a Three-Dimensional Medium

Ágota Tóth,\* Bernadett Veisz, and Dezső Horváth\*

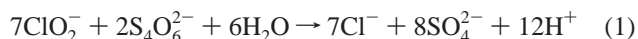
*Department of Physical Chemistry, József Attila University, P.O. Box 105, Szeged H-6701, Hungary*

*Received: January 24, 1998; In Final Form: May 13, 1998*

Lateral instability in reaction–diffusion fronts of the chlorite oxidation of tetrathionate is studied experimentally in three dimensions. A simple two-variable model based on the empirical rate law of the reaction is utilized to reproduce the experimental observations. The onset of instability does not change by extending the system from two to three dimensions; the natural wavelength associated with the cellular structure, however, slightly decreases.

Spatiotemporal pattern formation in reaction–diffusion systems of chemical reactions with a positive feedback has been studied extensively both experimentally and theoretically.<sup>1–3</sup> Diffusion-driven instability of a homogeneous state may lead to Turing patterns in the form of stripes or spots<sup>4–6</sup> and that of bistable states may result in replicating spots<sup>7</sup> or labyrinthine patterns.<sup>8</sup> In these systems the components have different diffusional length scales so that the autocatalytic species will have the lowest diffusivity. The experimental studies have generally been confined to thin layers, where the extent of the system in the third dimension is smaller than the wavelength associated with the patterns formed. This direction, however, has allowed the supply of reactants from a reservoir as the systems have been typically investigated in continuously fed unstirred reactors. In closed systems the study of temporarily formed patterns may be carried out in a three-dimensional medium with conditions identical to those required in two-dimensional thin layers. Reaction–diffusion fronts of reactions with a positive feedback in closed systems may give rise to pattern formation when lateral instability of planar fronts results in cellular structures. Flames of combustion may yield these structures as temperature plays an autocatalytic role via the Arrhenius kinetics of the exothermic reaction.<sup>9</sup> Under isothermal conditions, two examples of autocatalytic reactions exhibiting lateral instability are known: the iodate oxidation of arsenous acid catalyzed by iodide<sup>10</sup> and the acid-catalyzed

reaction of chlorite with tetrathionate in slight chlorite excess<sup>11,12</sup> given as



The necessary slower diffusivity of the autocatalyst is generally achieved by partial immobilization, which is accomplished by binding the hydrogen ions to carboxylate groups incorporated in a polyacrylamide/polymethacrylate hydrogel for reaction 1. In this work, we present for the first time how this instability of planar fronts develops to yield three-dimensional cellular structures. The experimental observations are then compared with the results of modeling calculations based on the empirical rate law of the reaction.

Reagent grade chemicals (Aldrich, Reanal) were used throughout the experiments except for sodium chlorite, which was recrystallized twice<sup>13</sup> to achieve a purity of 99.5%. Cross-linked polyacrylamide hydrogel copolymerized with various amounts of sodium methacrylate<sup>12</sup> served as a convection-free reaction medium and a binder for hydrogen ions via reversible protonation of the carboxylate groups of the polymer. The three-dimensional medium was constructed from quasi two-dimensional gel sheets, since a single block of hydrogel would require an experimentally unreasonable time for loading the reactant solution homogeneously. For each experiment 45 pieces of 4.5 × 4.5 × 0.1 cm<sup>3</sup> thin gels were cut and soaked in 800 mL of

**TABLE 1: Composition of Reactant Solutions**

[K <sub>2</sub> S <sub>4</sub> O <sub>6</sub> ]/M	0.005
[NaClO <sub>2</sub> ]/M	0.02
[NaOH]/M	0.001
[CH <sub>3</sub> COONa]/M	0.0015–0.0225
[congo red]/(g cm <sup>-3</sup> )	0.0004

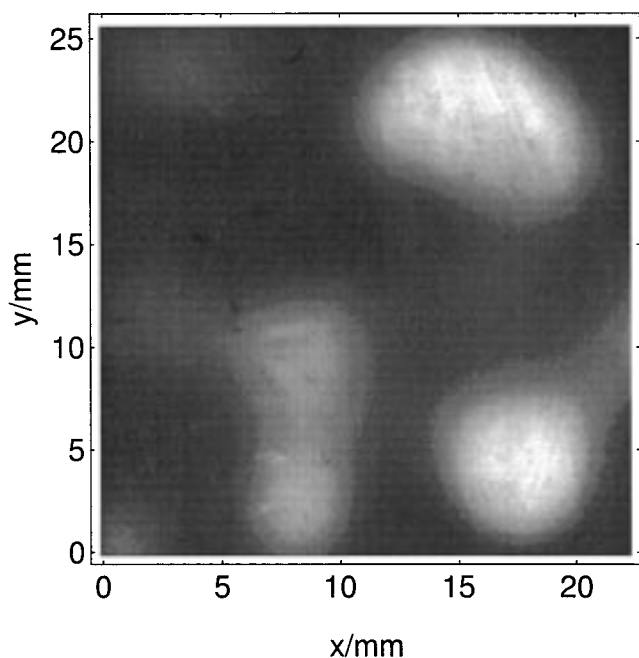


**Figure 1.** Image of a cellular front in a slice of hydrogel taken 14.7 h after initiation at high methacrylate content ( $c_M = 21$  mM). The gel sheet is 24.5 mm from the place of initiation, and only the inner section of the slice is shown where the inevitable edge effects are negligible. Lighter regions correspond to the product mixture behind, and darker ones to the reactant mixture ahead, of the front.

the reactant solution (for composition, see Table 1) for 30 min with vigorous stirring to provide a homogeneous loading of the gelled medium. The reactant solution contained sodium acetate in various concentrations to ensure a constant change of pH over the reaction, visualized by congo red indicator, and sodium hydroxide to prevent self-initiation. The gel slices were then wiped off thoroughly to remove excess liquid from the surface and piled tightly to form a column of ca. 4.5 cm in height. A front was initiated by placing a slightly acidic gel containing the product mixture on the top, and the reaction medium was covered to prevent evaporation. After 2–15 h, the slices were separated and the individual pieces were photographed with a black and white CCD camera connected to a computer-controlled imaging system. The visualization was enhanced by a broad-band filter ( $\lambda = 509$  nm).

Upon initiation, a reaction–diffusion front forms along the interface between the top gel sheet containing the product mixture and the next containing the reactant mixture, which then propagates across the gel slices. The whole medium can be considered isotropic, since fronts travel across the thin gels at the same velocity as that along them within experimental errors. The measured velocity of propagation decreases on increasing the methacrylate content of the medium and is in good agreement with previous experiments carried out in two-dimensional systems.<sup>12</sup>

In gels with low concentration of methacrylate, where the autocatalyst hydrogen ions have high apparent diffusion coefficient, the front retains its planar symmetry. Upon separation of the medium, this front structure then yields two types of individual gel sheets: one containing the reactant mixture and

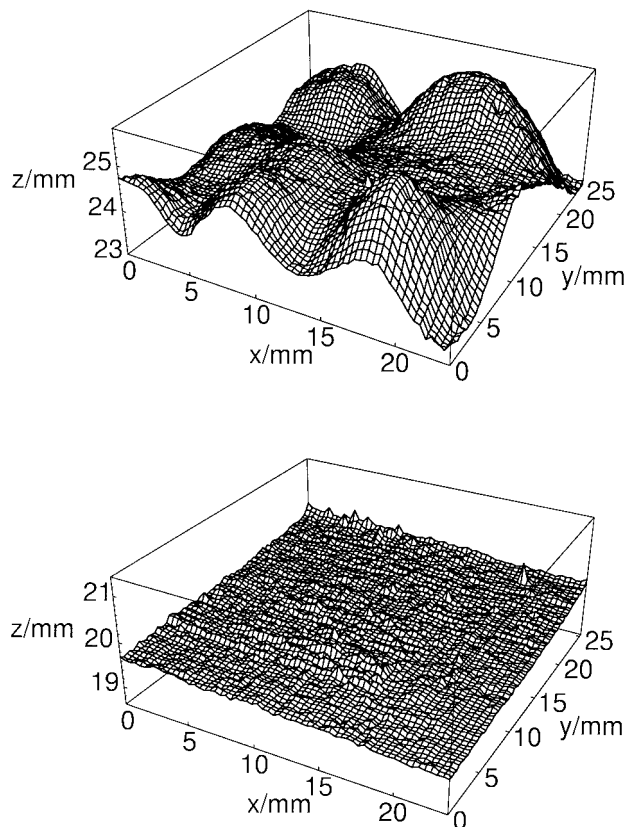


**Figure 2.** Position of the front constructed from images including that in Figure 1 (top), and a stable planar front developed at low methacrylate content ( $c_M = 9$  mM) at  $t = 3.5$  h (bottom).

the other the product mixture. Upon increasing the methacrylate content, the hydrogen ions are immobilized to a greater extent, resulting in the loss of stability of the planar front. The developed cellular front structure clearly appears upon inspection of the separated gel sheets. They have low gray-scale values homogeneously ahead and high gray-scale values behind the front much like in the case of planar fronts. In addition to slices containing only the reactant or the product mixture, there are several gel sheets intercepting the cellular front, in which the individual cells appear as lighter spots in the reactant zone as shown in Figure 1. The spots grow in size toward the back of the front and finally coalesce where the cells join to form a homogeneous product zone. Considering that light regions represent the acidic product mixture behind the front and dark areas the reactant mixture ahead, the position of the front in areas with intermediate gray-scale values can be determined by interpolation: the maximum in the gray scale corresponds to a position at the bottom of the gel while the minimum to that at the top with respect to the direction of propagation. The full three-dimensional structure of the front at higher resolution than the thickness of a single gel can then be constructed by superimposing the finer structures obtained from the gel sheets (see Figure 2). The same procedure utilized for experiments with low methacrylate content reveals the stable planar front shown in Figure 2 as well. By systematically varying the methacrylate concentration  $c_M$ , planar fronts lose stability at  $9 \text{ mM} < c_M < 12 \text{ mM}$ , representing 30–40% binding of the autocatalyst, which agrees well with the results of former experiments carried out in thin gels.<sup>12</sup> The naturally selected wavelength, however, decreases by ca. 10% and the estimated amplitude of the front is lowered by almost 50% on expanding the system from two to three spatial dimensions.

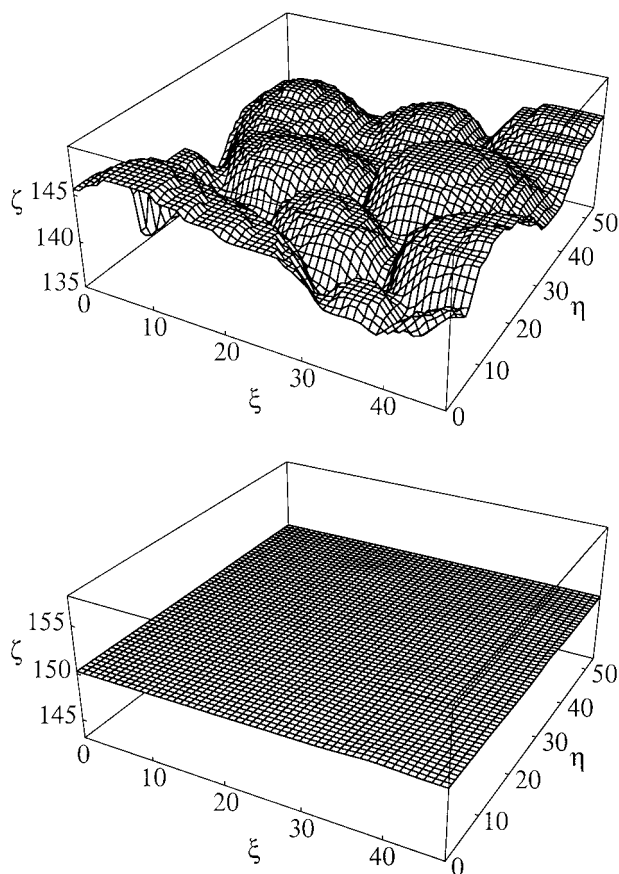


**Figure 3.** Calculated fronts upon integration of eq 2 at  $\tau = 300$  (top) and at  $\tau = 80$  (bottom) at methacrylate content given in Figures 1 and 2. The area corresponds to that of the front shown in Figure 2.

A two-variable model based on the empirical rate law determined for reaction 1<sup>14</sup> has been developed to describe the observed instability in two dimensions<sup>12,13</sup>

$$\frac{\partial \alpha}{\partial \tau} = \nabla^2 \alpha - \alpha \beta^2 (\kappa + 7\alpha) \quad (2a)$$

$$\frac{\partial \beta}{\partial \tau} = \frac{\delta \nabla^2 \beta}{\sigma} + \frac{6\alpha \beta^2 (\kappa + 7\alpha)}{\sigma} \quad (2b)$$

where  $\alpha = [\text{S}_4\text{O}_6^{2-}]/[\text{S}_4\text{O}_6^{2-}]_0$  and  $\beta = [\text{H}^+]/[\text{S}_4\text{O}_6^{2-}]_0$  are the relative concentrations of the limiting reactant tetrathionate and the autocatalyst hydrogen ion with respect to the initial concentration of tetrathionate ahead of the front  $[\text{S}_4\text{O}_6^{2-}]_0$ . The ratio of the diffusion coefficients is defined as  $\delta = D_{\text{H}^+}/D_{\text{S}_4\text{O}_6^{2-}}$ , the relative chlorite excess as  $\kappa = 2[\text{ClO}_2^-]/[\text{S}_4\text{O}_6^{2-}]_0 - 7$ , and the dimensionless space and time coordinates as  $\nabla^2 \equiv \partial^2/\partial \xi^2 + \partial^2/\partial \eta^2 + \partial^2/\partial \zeta^2 = (k[\text{S}_4\text{O}_6^{2-}]_0^3/D_{\text{S}_4\text{O}_6^{2-}})^{-1}(\partial^2/\partial x^2 + \partial^2/\partial y^2 + \partial^2/\partial z^2)$  and  $\tau = k[\text{S}_4\text{O}_6^{2-}]_0^3 t$  with  $k = 7.28 \times 10^4 \text{ M}^{-3} \text{ s}^{-1}$  being the rate constant<sup>13</sup> of reaction 1. The coefficient  $\sigma = 1 + c_{\text{M}}K_{\text{d}}/[\text{S}_4\text{O}_6^{2-}]_0^2/(K_{\text{d}}/[\text{S}_4\text{O}_6^{2-}]_0 + \beta)^2$  with dissociation constant of the carboxylic acid groups  $K_{\text{d}}$  accounts for the decrease of the effective diffusion coefficient of the hydrogen ion upon increasing the methacrylate content of the gel  $c_{\text{M}}$ . The partial differential equations of eq 2 were numerically solved by using an explicit Euler method on a  $91 \times 91 \times 101$  grid with no-flux boundary conditions and the Laplacian approximated as<sup>15</sup>

$$\nabla^2 \alpha_{i,j,k} \approx L_{\alpha,i,j,k} = \frac{1}{6h^2} \sum_{p=-1, q=-1, r=-1}^{p=1, q=1, r=1} a_{p,q,r} \alpha_{i+p, j+q, k+r} \quad (3)$$

where  $h$  is the spatial resolution of the grid. The coefficients  $a_{p,q,r}$  are taken as

$$(a_{p,q,-1}) = (a_{p,q,1}) = \begin{pmatrix} 0 & 1 & 0 \\ 1 & 2 & 1 \\ 0 & 1 & 0 \end{pmatrix}, \quad (a_{p,q,0}) = \begin{pmatrix} 1 & 2 & 1 \\ 2 & -2 & 2 \\ 1 & 2 & 1 \end{pmatrix} \quad (4)$$

resulting in an error of  $O(h^2)$  for the Laplacian.<sup>15</sup> A grid spacing of  $h = 0.9$  with  $\Delta \tau = 0.01$  was used at constant  $\delta = 1$ . For comparison with the experiments  $K_{\text{d}} = 10^{-5}$  and  $D_{\text{S}_4\text{O}_6^{2-}} = 2 \times 10^{-5} \text{ cm}^2 \text{ s}^{-1}$  without further adjustments were utilized to determine the length scales.<sup>12</sup> During the calculations, the concentration field on the grid was shifted back periodically to keep the front position in the center.

The initially imposed random noise in the planar front decays for  $c_{\text{M}} \leq 9 \text{ mM}$  as shown in Figure 3. By further increasing the methacrylate concentration, the planar front loses stability leading to the formation of a cellular structure illustrated in Figure 3. Similarly to the experimental observations, the onset of instability remains unchanged, while the natural size of individual cells decreases as the system is extended to three dimensions. The results of the calculations are in good agreement with those of the experiments since the calculated front profiles in Figure 3 represent the same extent of binding for the autocatalyst and the same area as in the experiments in Figure 2; only the top of the cells seem flatter in the calculations owing to the coarseness of the grid.

In conclusion, we have shown diffusion-driven lateral front instability in an isothermal chemical system for the first time in a three-dimensional medium. The simple two-variable reaction–diffusion model based on the empirical rate law clearly reproduces the cellular front structure observed in the experiments. The frontal patterns developed exhibit striking similarities to those found in three-dimensional cellular flames.<sup>9,16</sup>

**Acknowledgment.** A.T. is grateful to the Hungarian Science Foundation for financial support (OTKA D24071). D.H. thanks the Foundation for Hungarian Higher Education and Research for a Magyary Zoltán Fellowship.

## References and Notes

- (1) Nicolis, G.; Prigogine, I. *Self-Organization in Nonequilibrium Chemical Systems*; Wiley: New York, 1977.
- (2) Murray, J. D. *Mathematical Biology*; Springer: Berlin, 1989.
- (3) Kapral, R.; Showalter, K., Eds.; *Chemical Waves and Patterns*; Kluwer: Dordrecht, 1995.
- (4) Castets, V.; Dulos, E.; Boissonade, J.; De Kepper, P. *Phys. Rev. Lett.* **1990**, *64*, 2953.
- (5) Ouyang, Q.; Swinney, H. L. *Nature (London)* **1991**, *352*, 610.
- (6) Epstein, I. R.; Lengyel, I.; Kádár, S.; Kagan, M.; Yokoyama, M. *Physica A* **1992**, *188*, 26.
- (7) Lee, K. J.; McCormick, W. D.; Pearson, J. E.; Swinney, H. L. *Nature (London)* **1994**, *369*, 215.
- (8) Lee, K. J.; McCormick, W. D.; Ouyang, Q.; Swinney, H. L. *Science* **1993**, *261*, 192.
- (9) Sabathier, F.; Clavin, P. *Prog. Astronaut. Aeronaut.* **1981**, *76*, 246.
- (10) Horváth, D.; Showalter, K. *J. Chem. Phys.* **1995**, *102*, 2471.
- (11) Tóth, Á.; Lagzi, I.; Horváth, D. *J. Phys. Chem.* **1996**, *100*, 14837.
- (12) Horváth, D.; Tóth, Á. *J. Chem. Phys.* **1998**, *108*, 1447.
- (13) Tóth, Á.; Horváth, D.; Siska, A. *J. Chem. Soc., Faraday Trans.* **1997**, *93*, 73.
- (14) Nagypál, I.; Epstein, I. R. *J. Phys. Chem.* **1986**, *90*, 6285.
- (15) Dowle, M.; Mantel, R. M.; Barkley, D. *Int. J. Bif. Chaos* **1997**, *7*, 2529.
- (16) Sivashinsky, G. I. *Annu. Rev. Fluid Mech.* **1983**, *15*, 179.